Atmospheric Research 217 (2019) 198–207

Contents lists available at ScienceDirect

Atmospheric Research

journal homepage: www.elsevier.com/locate/atmosres

Study on pollution behavior and sulfate formation during the typical haze event in Nanjing with water soluble inorganic ions and sulfur isotopes

Ziyan Guo[a,b], Qingjun Guo[c], Shanli Chen[a,d], Bin Zhu[d], Yanlin Zhang[e], Jianghua Yu[a,b], Zhaobing Guo[b,*]

[a] Collaborative Innovation Center of Atmospheric Environment and Equipment Technology, Nanjing 210044, China
[b] School of Environmental Science and Engineering, Nanjing University of Information Science & Technology, Nanjing 210044, China
[c] Center for Environmental Remediation, Institute of Geographic Sciences and Natural Resources Research, Chinese Academy of Sciences, Beijing 100101, China
[d] School of Atmospheric physics, Nanjing University of Information Science & Technology, Nanjing 210044, China
[e] Yale-NUIST Center on Atmospheric Environment, Nanjing University of Information Science & Technology, Nanjing 210044, China

ARTICLE INFO

Keywords:
Haze
Water soluble inorganic ions
Sulfur isotope
Sulfate formation

ABSTRACT

The typical haze event in Nanjing was selected to study pollution behavior and sulfate formation by field measurement. Based on the concentrations of water soluble inorganic ions in $PM_{2.5}$, pollution characteristics of the haze were investigated with phase clustering analysis. Besides, $\delta^{34}S$ values of SO_2 and sulfate in $PM_{2.5}$ were determined in order to explore sulfur sources and sulfate formation. The result showed that $PM_{2.5}$ pollution during the haze event was significantly serious, which was mainly from coal combustion, vehicle exhaust emission and biomass burning. Sulfate formation was attributed to aqueous phase sulfur oxidation reactions promoted by high relative humidity and NO_2 concentration under the alkaline condition. The color of sky on 22 Dec. was ascribed to the combination of sunset glow and fine particles in high-moisture atmosphere. $\delta^{34}S$ values of SO_2 are found to be lower than those of sulfate in $PM_{2.5}$ indicating there was presence of sulfur isotopic fractionation during SO_2 oxidation. The average contribution of SO_2 homogenous oxidation to sulfate was about 51.2% during the haze events. The ratio of SO_2 heterogeneous and homogeneous oxidation to sulfate was mainly attributed to the concentrations of gaseous pollutants (NO_2, SO_2 and O_3) and relative humidity of the atmosphere.

1. Introduction

$PM_{2.5}$ is a particulate matter with aerodynamics equivalent diameter ≤ 2.5 μm (GB3095–2012). Haze is defined as a pollution phenomenon which cuts atmospheric visibility to < 10 km due to the complex materials suspended in the atmosphere (China Meteorological Administration, 2010). Generally, haze is mainly related to high $PM_{2.5}$ concentration, relative humidity (RH) < 90% and stable meteorological condition (Peng et al., 2016; Feng et al., 2016; Yuan et al., 2015). Chen et al. (2012) proposed a parameterization of light extinction for low visibilities on hazy days and found that a high aerosol volume concentration was responsible for low visibility. Usually, $PM_{2.5}$ possesses profound impacts on human and ecosystem health, weather and climate change (Cheng et al., 2013). Although the government took great efforts to control air pollution (Cai et al., 2017; Wang et al., 2017a, 2017b), China has been suffering from haze pollution nowadays due to the massive emission of particulate matter and gaseous pollutants (Jiang et al., 2016). There exists the heaviest haze pollution observed in four regions in China: Beijing-Tianjin-Hebei (Tan et al., 2016; Gao et al., 2015; Guo et al., 2014), Yangtze River Delta (Cheng et al., 2013; Shen et al., 2015), Pearl River Delta (Tao et al., 2014) and Sichuan Basin (Wang et al., 2017a, 2017b). However, the formation mechanism of heavy haze event remains uncertain in China (Zhang et al., 2015).

Nanjing, located in Yangtze River Delta, is one of the biggest cities in China with an area of 6597 km^2 and permanent resident population > 8.2 millions. The annual average temperature and precipitation are about 15.4 °C and 1106 mm, respectively. Generally, the pollution of particulate matter in Nanjing is rather serious (Wang et al., 2012). Li et al. (2016) measured water soluble inorganic ions (WSIIs) and metal elements during the haze-fog events in Nanjing and identified emission sources as road dust, coal combustion and steel industry. Kong et al. (2015) studied the variation of PAHs in $PM_{2.5}$ during winter haze period in Nanjing, indicating that coal combustion, traffic emission,

* Corresponding author.
E-mail address: guozbnuist@163.com (Z. Guo).

https://doi.org/10.1016/j.atmosres.2018.11.009
Received 20 August 2018; Received in revised form 24 October 2018; Accepted 11 November 2018
Available online 14 November 2018
0169-8095/

industrial production and petroleum were main sources of PAHs. Wang et al. (2011) determined chemical compositions and size distribution of water soluble organic compounds in particles during a heavy haze caused by field burning in Nanjing and made clear the effect of straw burning on the haze.

Sulfate is one of the prevalent components of $PM_{2.5}$. It is controversial for rapid growth of sulfate concentration during the haze in China. Wang et al. (2016) and Cheng et al. (2016) believed that the presence of NO_2 was obviously favorable for SO_2 oxidation under the conditions of high RH and NH_3. However, Guo et al. (2017) insisted that SO_2 catalytic oxidation of metal ions was main sulfate formation process. Sulfur isotope can be used for tracing sulfur source and exploring sulfate formation (Xiao et al., 2014). Therefore, it is admirable to determine sulfur isotopic composition in $PM_{2.5}$ during the haze events. Nowadays, as an effective indicator, $\delta^{34}S$ has been adopted to identify sulfur sources of the atmosphere around the world. Ohizumi et al. (2014) monitored sulfur isotopic ratio in sulfate deposition for 28 years at Nagaoka indicating that $\delta^{34}S$ could be applied to perceive the change of emission sources. Han et al. (2016) used sulfur and oxygen isotopes to identify the sources of Beijing aerosol suggesting that biogenic sulfur emission in summer and the increasing coal combustion in winter were the main contributions to aerosol. Sakata et al. (2013) studied $\delta^{34}S$ value in aerosol from Japan Sea coast and concluded sulfur isotope was a tracer of emission during coal combustion. Besides, Leung et al. (2001) and Sinha et al. (2008) found that $\delta^{34}S$ in aerosol could be employed to distinguish the mixing processes and transport pathways of sulfur-containing pollutants in the atmosphere.

In the contribution, we chose the typical haze events in Nanjing from 21 Dec. 2015 to 1 Jan. 2016 to study pollution characteristics and sulfate formation. Especially, a scarcely purple sky during the haze event was observed at 17:00 on 22 Dec. 2015. Many local and national news outlets reported this unusual haze event (http://news.xinhuanet.com/local/2015-12/23/c_128559783.htm). It is unclear whether there existed the difference in pollution behaviors of this haze compared to other haze events. In addition, sulfate formation during the haze was usually complicated in China. Single component analysis hardly reflected pollution characteristics. Therefore, except the WSIIs, $\delta^{34}S$ values of dissolved sulfate and SO_2 were synchronously determined to make clear the sources of $PM_{2.5}$ and sulfate formation during the haze event.

2. Materials and methods

2.1. Sampling site

$PM_{2.5}$ and SO_2 samples were collected on the roof of the library in Nanjing University of Information Science & Technology (NUIST, 32.1° N, 118.5° E), which is about 35 m above the ground. The sampling site of NUIST in Nanjing, China is depicted in Fig. 1. The site, located at the side of Ningliu Road, is close to Nanjing chemical industry park. There are presence of many large-scale steel plants, petrochemical companies and thermal power plants, which release massive exhaust gases and particles. In addition, there exists a small amount of rice farmland around the sampling site.

2.2. Determination of particle number and spectral distribution

Wide-range Particle Spectrometer (1000XP, MSP Co., USA) was used to determine number concentration and spectral distribution of aerosol particles. The sampling flows of Differential Mobility Analyzer and Laser Particle Spectrometer were 0.3 and 0.70 $L{\cdot}min^{-1}$, respectively. The time resolution was set at 5 min.

2.3. Sample collection

$PM_{2.5}$ and SO_2 were collected using a modified sampler (TH-1000H, Tianhong Co., Wuhan) with a flow rate of 1.05$m^3{\cdot}min^{-1}$ from 9 am to 9 pm per day from 21 Dec. 2015 to 1 Jan. 2016, which covered a complete process of haze pollution. The double sampling frames were installed in the sampler slot. The upper sampling frame was used to collect $PM_{2.5}PM_{2.5}$, while the lower sampling frame was adopted to gather SO_2. Before $PM_{2.5}$ and SO_2 sampling, the sampler was usually calibrated to ensure the accuracy.

$PM_{2.5}$ and SO_2 were sampled with quartz filters (203 × 254 mm, Munktell, Sweden) and glass fiber filters (203 × 254 mm, Tisch Enviroment INC, USA), respectively. Before $PM_{2.5}$ and SO_2 sampling, the filters were firstly incinerated in a muffle furnace at 450 °C for 4 h to avoid the influence of organic matters and moisture. Then, quartz filters were directly placed in the desiccators at room temperature. The glass fiber filters were soaked in the solution of 2% K_2CO_3 and 2% glycerol for 2 h. After being dried in DGG-9070A electric oven, the filters were kept in the desiccators for 24 h at room temperature. While SO_2 sampling, it can be absorbed in alkaline-soaked glass fiber filters and transformed into SO_3^{2-} and HSO_3^- immediately.

The sampled filters were reserved in a refrigerator for chemical analysis. During the samples treatment, H_2O_2 solution was used to oxidize SO_3^{2-} and HSO_3^- into sulfate.

2.4. WSIIs analysis

After the dissolution of 1/32 sampled filter with Milli-Q water and the filtration with 0.22 μm membrane, the concentrations of the WSIIs (Na^+Na^+, $NH_4^+NH_4^+$, K^+, Ca^{2+}, $Mg^{2+}Mg^{2+}$, Cl^-, NO_3^- and SO_4^{2-}) in $PM_{2.5}$ were measured by using ICS-3000 and ICS-2000 Ion Chromatography (Dinoex, USA). The detection limit of each ion was lower than 0.015 $\mu g{\cdot}m^{-3}$.

2.5. Sulfur isotopic analysis

Sulfur isotopic composition was analyzed in State Key Laboratory of Biogeology and Environmental Geology in China University of Geosciences (Wuhan). Elemental analyzer (EA, Flash 2000, Thermo) and isotopic mass spectrometer (IRMS, Delta V Plus, Finningan) were used to determine $\delta^{34}S$ of sulfate in $PM_{2.5}$. Specifically, 1/4 sampled filters were shredded and soaked overnight in 200 mL Milli-Q water. Dissolved sulfate in $PM_{2.5}$ was precipitated as $BaSO_4$ by adding 3 mL 1 $mol{\cdot}L^{-1}$ $BaCl_2$. The precipitate was then separated by 0.22 μm acetate membrane and rinsed with 150 mL Milli-Q water to remove Cl^-. Finally, the precipitate was transferred to ceramic crucible and combusted at 800 °C in muffle furnace for 2 h to acquire high-purity $BaSO_4$ powder. $BaSO_4$ was converted into SO_2 in EA in the presence of Cu_2O. SO_2 from EA was ionized and $\delta^{34}S$ value was measured using IRMS. The result was with respect to international standard V-CDT and the accuracy was better than ± 0.2‰.

The determination of the WSIIs and sulfur isotopic composition was carried out in duplicate and the average values were used for data analysis.

2.6. Phase clustering analysis

Phase clustering analysis can be used to describe the similarity of different sample clusters. In this study, we used three phases clustering analysis to explore the distribution of the WSIIs in $PM_{2.5}$. We firstly divided the WSIIs into three phases according to different sources. On this basis, the proportions of three phases were calculated. The proportion in different $PM_{2.5}$ samples might have a certain discrepancy, but the samples with similar proportion would assemble together.

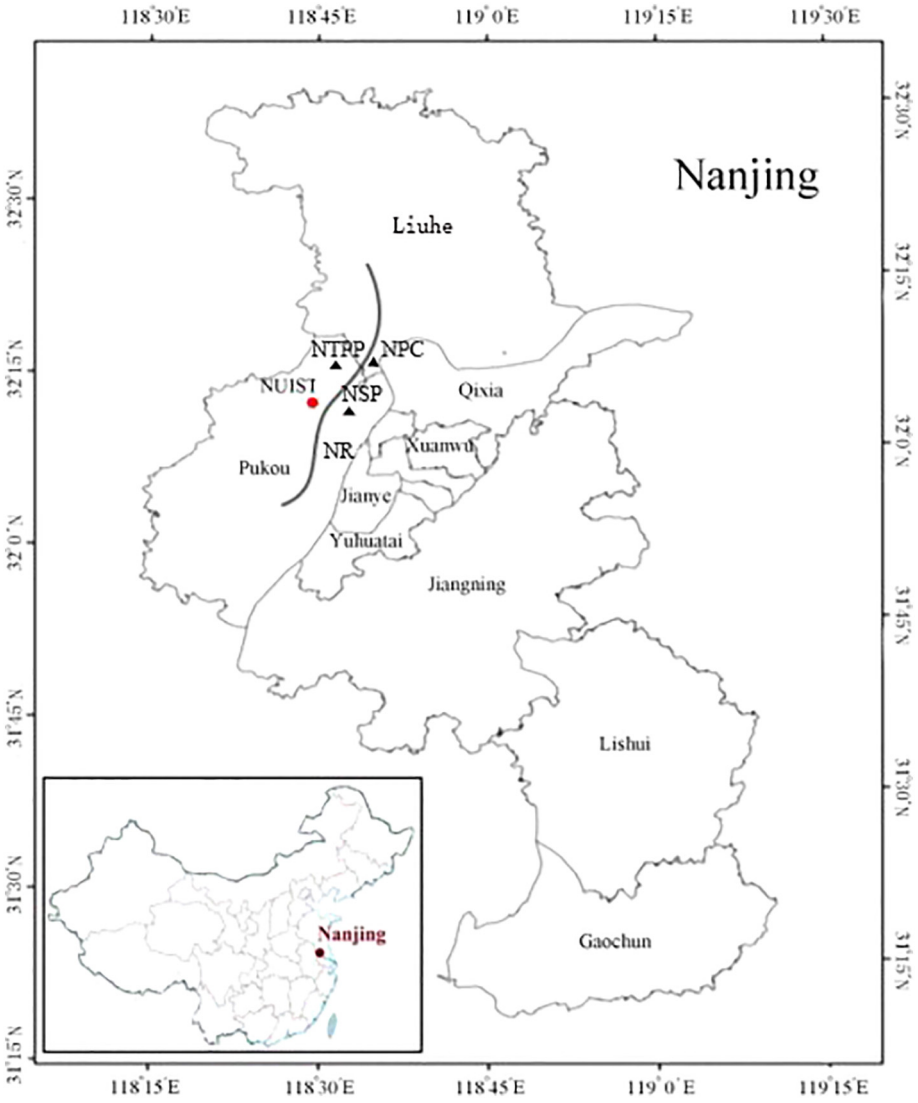

Fig. 1. Sampling site of NUIST in Nanjing, China. NSP: Nanjing steel plants; NTPP: Nanjing thermal power plants; NPC: Nanjing petrochemical company; NR: Ningliu Road.

3. Results and discussion

3.1. Pollution behavior of $PM_{2.5}$ during the haze event

3.1.1. $PM_{2.5}$ concentration

The mass concentration and number concentration of $PM_{2.5}$ during the haze events are shown in Fig. 2. It can be observed that mass concentrations of $PM_{2.5}$ ranged from 40.03 to 233.43 $\mu g \cdot m^{-3}$ with an average and standard deviation of 144.67 ± 54.12 $\mu g \cdot m^{-3}$, which is 1.93 times of the Second Grade National Ambient Air Quality Standard (75 $\mu g \cdot m^{-3}$) and 4.13 times of the First Grade National Ambient Air Quality Standard (35 $\mu g \cdot m^{-3}$) (GB3095–2012). Meanwhile, mass concentrations of $PM_{2.5}$ were beyond the safety standard of World Health Organization (10 $\mu g \cdot m^{-3}$) during the observation period. In addition, we noted that average mass concentration of $PM_{2.5}$ during the haze events was higher than those in Hong Kong (55.50 $\mu g \cdot m^{-3}$, Cheng et al., 2015), Guangzhou (76.80 $\mu g \cdot m^{-3}$, Tao et al., 2014), Xiamen (86.20 $\mu g \cdot m^{-3}$, Zhang et al., 2012), Beijing (115.80 $\mu g \cdot m^{-3}$, Hu et al., 2014) and Xi'an (142.60 $\mu g \cdot m^{-3}$, Wang et al., 2015), indicating that $PM_{2.5}$ pollution was very serious. As indicated in Fig. 2, mass concentrations of $PM_{2.5}$ during the haze event markedly fluctuated. The highest $PM_{2.5}$ concentration occurred on 22 Dec. 2015 with a value at 233.43 $\mu g \cdot m^{-3}$, then significantly decreased to 125.39 $\mu g \cdot m^{-3}$ on 23 Dec. Besides, the lowest $PM_{2.5}$ concentration was found to be 40.03 $\mu g \cdot m^{-3}$ on 27 Dec. According to weather conditions of Nanjing during the haze events in Fig. 3, high $PM_{2.5}$ concentration on 22 Dec. was related to low wind speed, the continuously static and stable weather made it difficult to spread for fine particles in the atmosphere, thereby causing the accumulation of different pollutants (Ueda et al., 2016; Cuhadaroglu and Demirci, 1997). Considering relative humidity at 85% and visibility < 2 km on 22 Dec., we inferred that there was presence of a heavy haze event on 22 Dec. It can be observed from Fig. 3 that the decrease of $PM_{2.5}$ concentration on 23 Dec. was due to the precipitation. The lowest $PM_{2.5}$ concentration on 27 Dec. was mainly ascribed to high wind speed, which was favorable for the diffusion of fine particles.

The number concentrations of $PM_{2.5}$ during the observation period varied from 6067.8 to 21,225.3 $\#\cdot cm^{-3}$ with an average and standard deviation of 13,165.7 ± 4714.7$\#\cdot cm^{-3}$ (Fig. 2). It is noteworthy that there existed the uncertainty between mass concentration and number concentration of $PM_{2.5}$. For instance, high mass concentration corresponded to the relatively high number concentration of $PM_{2.5}$ on 22 Dec. While on 29 Dec., there existed low mass concentration and rather high number concentration. Generally, mass concentration of $PM_{2.5}$ was mainly dominated by the larger particles, while number concentration of $PM_{2.5}$ was mainly affected by fine particles. Therefore, the

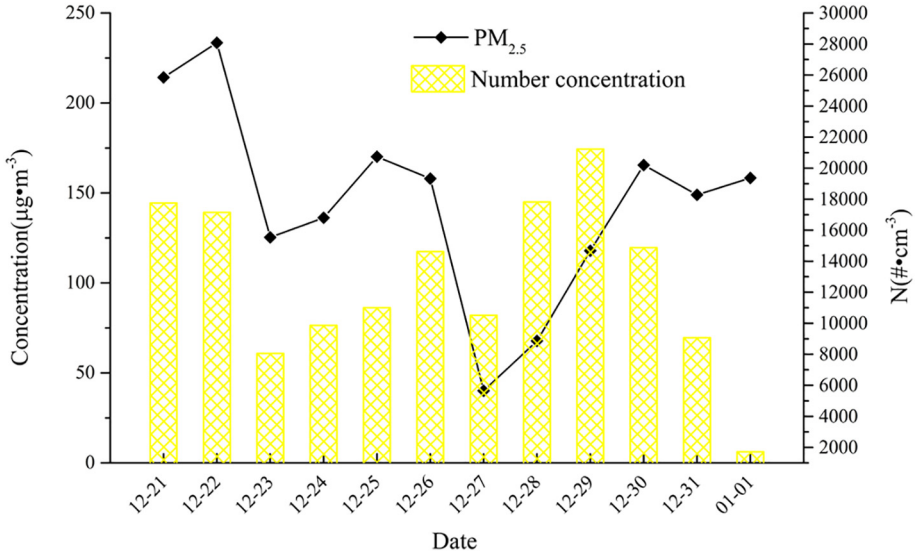

Fig. 2. The mass concentrations and number concentrations of $PM_{2.5}$ during the observation period.

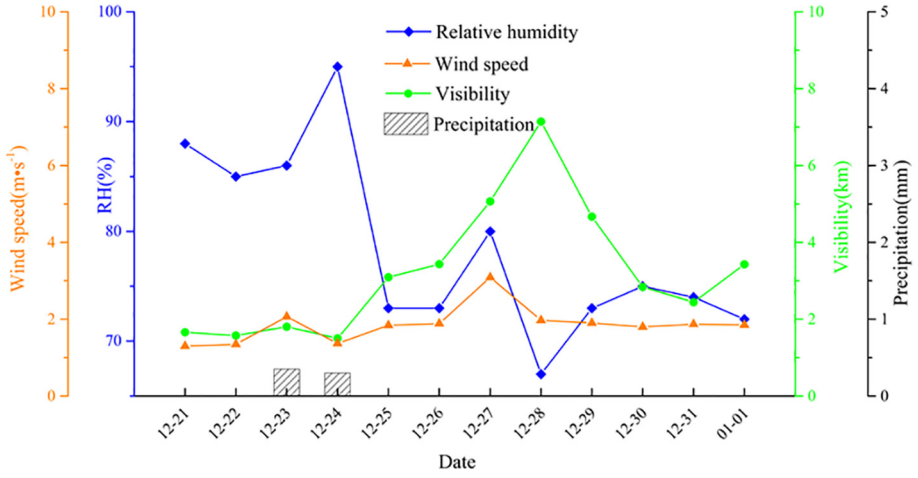

Fig. 3. The weather conditions during the observation period.

discrepancy between mass concentration and number concentration of $PM_{2.5}$ was chiefly ascribed to different particle number size distribution. As shown in Fig. 4, the particle number size distribution on 22 Dec. (Fig. 4a) mainly concentrated below 500 nm and peak value of number concentration at 150 nm was about 650 #·cm^{-3}. However, the particle number size distribution was below 400 nm and peak value of number concentration at 100 nm was about 800 #·cm^{-3} on 29 Dec. (Fig. 4b). This indicated that there were more superfine particles on 29 Dec. compared to those on 22 Dec. It is noted that there existed high relative humidity (85%) and lots of fine particles in the atmosphere on 22 Dec. When sunlight passed through small water drops and fine particles, it could be resolved into different kinds of monochromatic light, thereby causing the appearance of the sky color. Therefore, the color of sky on 22 Dec. was just a physical phenomenon from the combination of sunset glow with water drops and fine particles.

3.1.2. *WSIIs of $PM_{2.5}$*

The concentrations of WSIIs in $PM_{2.5}$ during the haze events are compared in Table 1 and concentration distribution for each ion is shown in Fig. 5. The average value and standard deviation of Na^+, $NH_4^+NH_4^+$, K^+, Ca^{2+}, $Mg^{2+}Mg^{2+}$, Cl^-, NO_3^- and SO_4^{2-} were 0.75 ± 0.40, 21.30 ± 10.51, 1.84 ± 0.89, 0.86 ± 0.30, 0.35 ± 0.26, 4.81 ± 2.67, 26.46 ± 11.51 and 19.01 ± 6.78 μg·m^{-3}, respectively. The predominant ions in $PM_{2.5}$ during the haze events were NO_3^-, NH_4^+ and SO_4^{2-}, accounting for 86.58% of the WSIIs. NO_3^- and SO_4^{2-} were the dominant anions, the concentrations of which were much higher compared to that of Cl^-. NH_4^+ was the most important cation in $PM_{2.5}$, the concentrations of K^+, Ca^{2+}, Na^+ and Mg^{2+} were relatively lower.

Three phases clustering analysis was used to interpret the distribution of the WSIIs in $PM_{2.5}$ during the haze events. NO_3^-, NH_4^+ and SO_4^{2-} were the typically secondary pollutants, there was presence of good correlations between NH_4^+ and NO_3^- (r = 0.87), NH_4^+ and SO_4^{2-} (r = 0.80), NO_3^- and SO_4^{2-} (r = 0.92). Considering NH_4^+ was mainly from nitrogen utilization, livestock's and the secondary formation of exhaust gas from fuel combustion and vehicle emission (Ge et al., 2011), NO_3^- was chiefly from the conversion of NO_x (Pastuszka and Wawroś, 2003) and SO_4^{2-} mainly came from coal combustion and the oxidation of SO_2 (Lu et al., 2010; Karthikeyan and Balasubramanian, 2006), we classified NH_4^+, $NO_3^-NO_3^-$ and SO_4^{2-} together as the first phase. Besides, it is known that K^+ was an indicator of biomass burning (Yang et al., 2015) and Cl^- was usually from coal combustion and biomass burning (Zhou et al., 2016). So we put K^+ and Cl^- together as the second phase. Finally, we defined Na^+, Mg^{2+} and Ca^{2+} as the third phase due to these ions were mainly from natural sources such as dust and sea salt. On this basis, three phases clustering

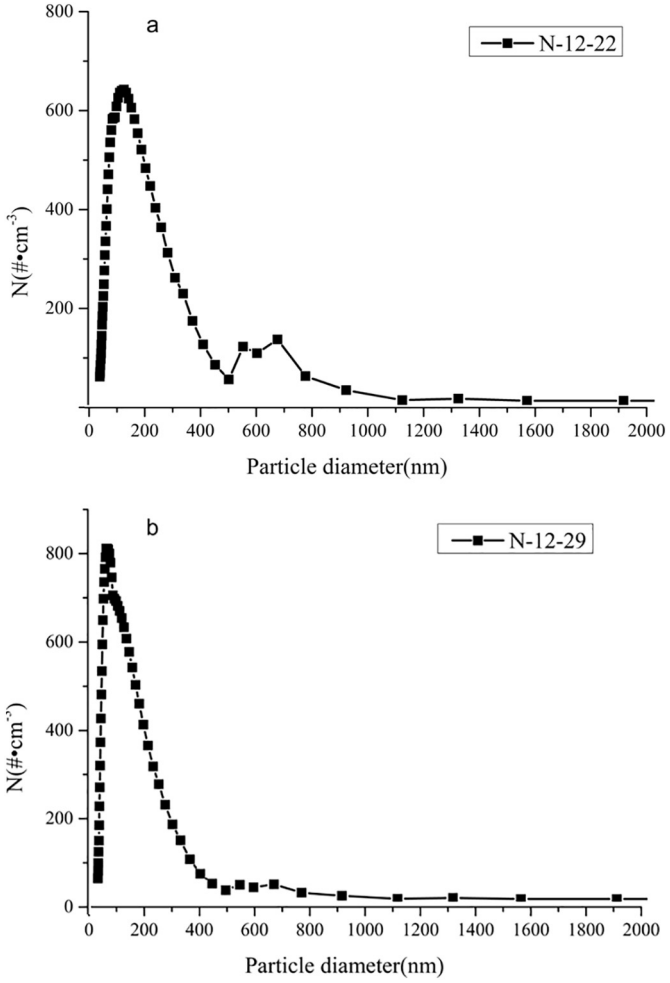

Fig. 4. The particle number size distribution on 22 and 29Dec.2015.

analysis was carried out and the results are shown in Fig. 6.

It is observed from Fig. 6 that twelve observation days of haze events can be divided into two categories named as a-I and a-II, respectively. The ten days of a-II concentrated on high level area of the secondary ions ($NH_4^+ + NO_3^- NO_3^- + SO_4^{2-}$), the average percent of which was as high as 89.39%. While the other two days of a-I was at low level area of the secondary ions with an average of 74.23%. In addition, there existed a good correlation between the secondary ions and $PM_{2.5}$ ($r = 0.94$) indicating that the secondary pollution during the haze events was relatively significant. For the phase of Na^+, Mg^{2+} and Ca^{2+}, a-I and a-II were at the similar level area. Ca^{2+} can be regarded as the indicators of dust (Duo et al., 2015; Cong et al., 2011; Sun et al., 2013) and Na^+ was mainly from sea salt. The negative correlation of $PM_{2.5}$ with Ca^{2+} $PM_{2.5}$withCa^{2+}($r = -0.42$) and Na^+ ($r = -0.33$) showed that the contribution of dust and sea salt to $PM_{2.5}$ was low in the heavily polluted atmosphere and high in the clean atmosphere. Therefore, the natural sources such as dust and sea salt had no obvious effect on $PM_{2.5}$ pollution during the haze events. It is pointed out that there existed a difference between a-I and a-II for the phase of K^+ and Cl^-. Compared with a-II (5.57%), a-I was at high level area of 15.82%. Besides, $PM_{2.5}$ had relatively high correlation coefficients with Cl^- ($r = 0.54$) Cl^-(r = 0.54)and K^+ ($r = 0.61$), which indicated that biomass burning was a source for$PM_{2.5}$ during the haze events.

As the main ions of $PM_{2.5}$, NO_3^-, SO_4^{2-} and NH_4^+ may constitute inorganic aerosol system with H_2O in the particle where NO_3^- and SO_4^{2-} can compete for NH_4^+ (Seinfeld and Pandis, 1998). Thus, it is favorable for studying their mutual relations to make clear the characteristics of the secondary pollution. Therefore, three phases clustering analysis of NO_3^-, SO_4^{2-} and NH_4^+ was conducted and the proportions of each ion in the system were calculated. The corresponding results are shown in Fig. 7. The whole observation days could be classified into three categories named as b-I, b-II and b-III, respectively. There existed a large difference in the proportions of three ions in the system. The proportions of SO_4^{2-}, NH_4^+ and NO_3^- in b-I followed a decreasing order with the values of 50.45%, 29.55% and 20.00%, respectively. However, the proportion of SO_4^{2-}, NH_4^+ and NO_3^- in b-II fit an increasing order with the values of 28.15%, 33.26% and 38.59%. In b-III, the proportions of SO_4^{2-}, NH_4^+ and NO_3^- were 29.70%, 21.89% and 48.41%, respectively. The discrepancies in the proportions of NO_3^-, SO_4^{2-} and NH_4^+ might be ascribed to the precursors from different pollution sources and the combination mode of NO_3^-, SO_4^{2-} with NH_4^+.

$[NO_3^-]/[SO_4^{2-}]$ has been used as an indicator to evaluate the importance of stationary and mobile sources (Arimoto et al., 1996). High $[NO_3^-]/[SO_4^{2-}]$ ratio (> 1) indicated the predominance of mobile sources over stationary sources. $[NO_3^-]/[SO_4^{2-}]$ value in b-I was 0.40 suggesting that stationary sources were at the more important position. While $[NO_3^-]/[SO_4^{2-}]$ values in b-II and b-III were 1.39 and 1.64, respectively, indicating that mobile sources made the more contribution to $PM_{2.5}$. NH_4^+ can be transformed into $(NH_4)_2SO_4$, NH_4HSO_4 and NH_4NO_3 via the reactions with NO_3^- and SO_4^{2-}. When NH_4^+ was in the forms of NH_4NO_3 and $(NH_4)_2SO_4$, the calculated $[NH_4^+] = 0.38[SO_4^{2-}] + 0.29[NO_3^- NO_3^-]$; While NH_4^+ was in the forms of NH_4NO_3 and NH_4HSO_4, the calculated $[NH_4^+] = 0.19[SO_4^{2-}] + 0.29[NO_3^-]$ (Kang et al., 2004). It is obtained that the correlation coefficient between the measured $[NH_4^+]$ during the haze events and the calculated $[NH_4^+]$ based on the first equation was 0.85. Similarly, the correlation coefficient between the

Table 1
The concentrations of the WSIIs in $PM_{2.5}$ and gaseous pollutants during the haze events ($\mu g \cdot m^{-3}$).

Date	Na^+	NH_4^+	K^+	Ca^{2+}	Mg^{2+}	Cl^-	NO_3^-	SO_4^{2-}	SO_2	NO_2	O_3
12–21	0.77	35.89	3.78	1.09	0.11	8.71	40.62	23.74	21	71	43
12–22	0.62	38.93	2.89	0.65	0.07	5.81	39.78	23.51	25	91	15
12–23	0.68	18.44	1.89	0.63	0.05	4.68	18.9	17.9	15	57	13
12–24	0.64	20.85	1.80	0.49	0.03	3.40	25.03	20.58	13	56	18
12–25	0.47	28.41	1.21	0.91	0.10	1.74	36.48	28.65	28	51	47
12–26	0.54	22.62	1.16	1.20	0.47	3.02	28.33	22.05	43	83	25
12–27	0.52	3.93	0.45	0.68	0.42	2.82	2.66	6.71	17	50	33
12–28	1.83	5.99	1.97	1.32	0.59	2.67	12.54	7.07	17	59	24
12–29	0.80	19.51	2.25	1.02	0.71	3.90	23.19	17.99	27	68	28
12–30	0.56	17.35	1.50	0.61	0.70	3.02	22.33	13.97	31	80	30
12–31	0.38	15.73	1.05	0.49	0.56	9.52	36.92	24.52	31	87	29
01–01	1.20	27.99	2.11	1.18	0.34	8.37	30.74	21.48	29	81	36
Average	0.75	21.30	1.84	0.86	0.35	4.81	26.46	19.01	24.75	69.50	28.42
SD	0.40	10.51	0.89	0.30	0.26	2.67	11.51	6.78	29	14.68	10.43

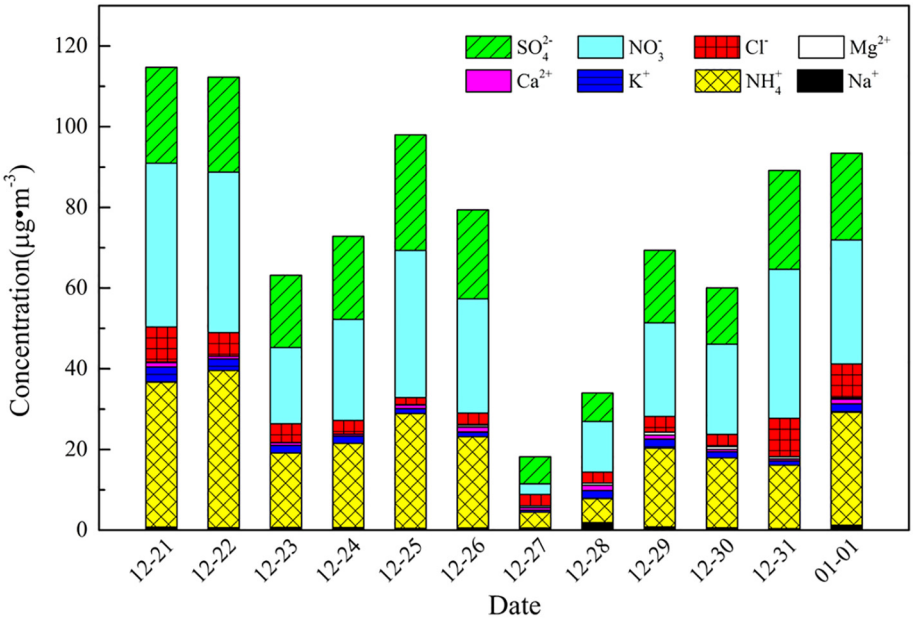

Fig. 5. The concentration distribution of WSIIs in $PM_{2.5}$.

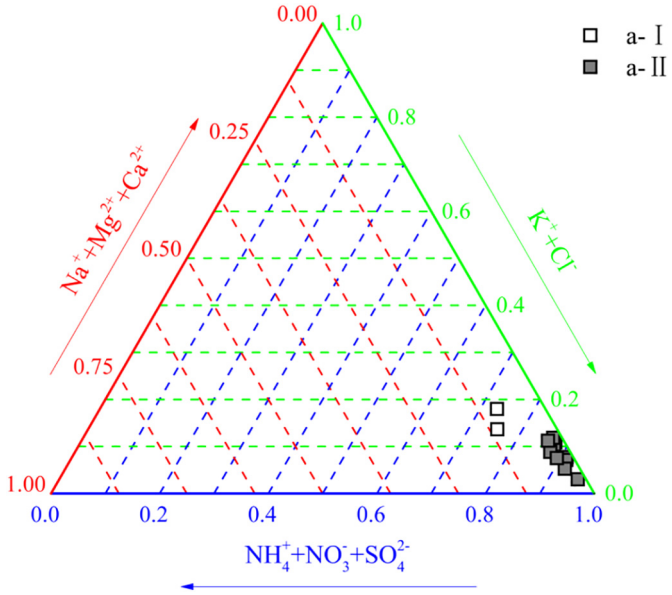

Fig. 6. Three phases clustering of WSIIs in $PM_{2.5}$.

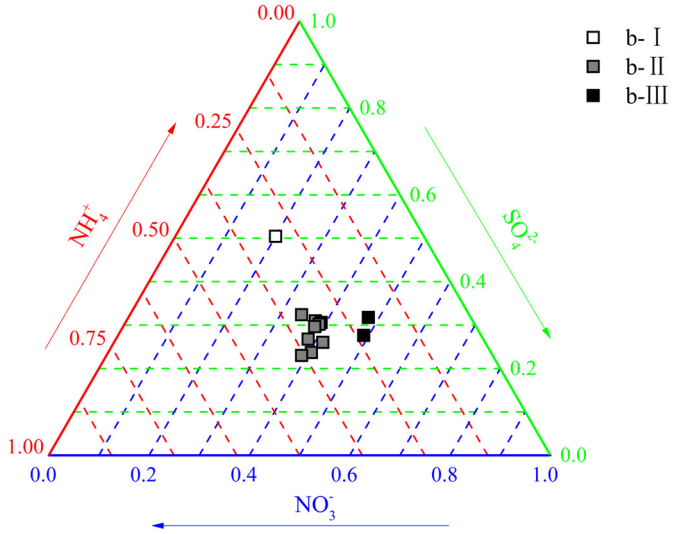

Fig. 7. Three phases clustering of NO_3^--SO_4^{2-}-NH_4^+ in $PM_{2.5}$.

measured [NH_4^+] and the calculated [NH_4^+] according to the second equation was 0.86. A good correlation between the measured [NH_4^+] and the two calculated [NH_4^+] indicated that NH_4^+ existed in the forms of $(NH_4)_2SO_4$, NH_4HSO_4 and NH_4NO_3 in $PM_{2.5}$ during the haze events.

High SO_4^{2-} and NO_3^- concentrations in $PM_{2.5}$ showed that there existed serious secondary pollution during the haze events. Besides, a good positive correlation between the concentrations of SO_4^{2-} and NO_3^- indicated that sulfate formation was accompanied by the increased NO_3^- concentration. This is mainly ascribed to SO_2 oxidation to sulfate in the presence of NO_2 under the alkaline condition. We studied the acid-base property of $PM_{2.5}$ using the ratio of anions (A) and cations (C) (Hassan and Khoder, 2017). A and C can be calculated by $A = NO_3^-/62 + SO_4^{2-}/48 + Cl^-/35.5$ and $C = Na^+/23 + NH_4^+/18 + K^+/39 + Mg^{2+}/12 + Ca^{2+}/20$, respectively. A/C values were generally lower than 1 indicating the alkalinity of $PM_{2.5}$ during the observation period. The lowest A/C value of 0.56 illustrated the strongest alkalinity on 22 Dec., which was favorable for SO_2 oxidation of high-concentration NO_2 (Hassan and Khoder, 2017; Sarwar et al., 2013). This can be confirmed by the results in Table 1.

Our observation was in agreement with Community Multiscale Air Quality (CMAQ) model simulation under NO_2-rich environment, which improved sulfate production up to 20% in wintertime (Sarwar et al., 2013). However, low NO_2 concentration (51 μg·m^{-3}) and high SO_4^{2-} content (28.65 μg·m^{-3}) were found on 25 Dec. According to RH and the concentrations of gaseous pollutants in Fig. 3 and Table 1, we inferred that this was related to high O_3 concentration (47 μg·m^{-3}) and low RH (38%), which was helpful for the photochemical reactions from SO_2 to sulfate. On the contrary, very low O_3 concentration and high RH resulted in large amounts of sulfate on 22, 26 and 31 Dec. This was mainly attributed to the presence of very high NO_2 concentration and the strong alkalinity of $PM_{2.5}$ in the atmosphere, which facilitated sulfate formation via aqueous phase sulfur oxidation reactions (Wang et al., 2016; Xie et al., 2015). This mechanism of sulfate formation was possibly dominated during the serious wintertime haze due to low O_3 concentration and the weak photochemical activity. Therefore, the

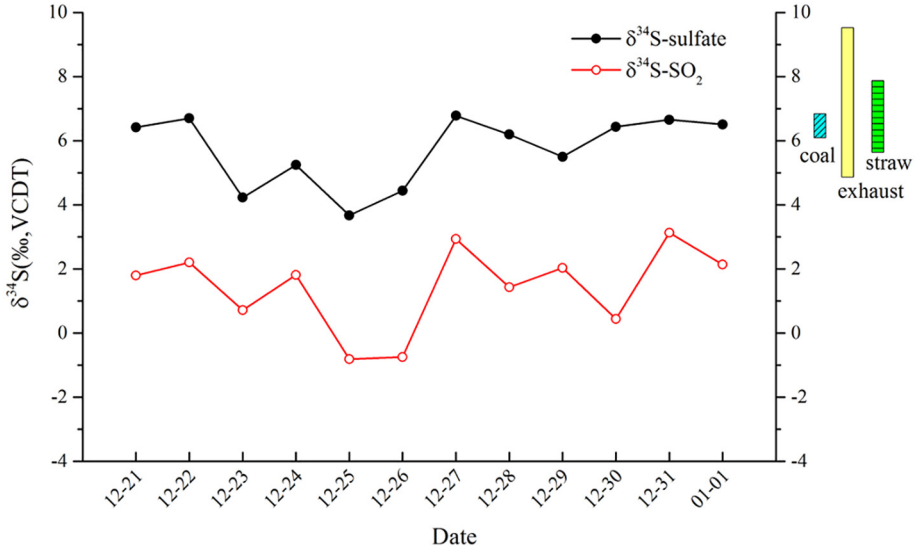

Fig. 8. The values of $\delta^{34}S\text{-}SO_4^{2-}$, $\delta^{34}S\text{-}SO_2$ and potential sulfur sources.

measured high NO_3^- concentrations were partly attributed to an enhanced heterogeneous conversion of NO_2 to NO_3^-. At the early stage of the haze events (21 Dec.), the conversion of SO_2 to sulfate was mainly controlled by photochemical processes and accompanied with aqueous reactions due to high O_3 concentration (43 μg·m^{-3}) and relatively high NO_2 concentration (71 μg·m^{-3}) and RH (55%). With the aggregation of the haze on 22 Dec., the highest concentrations of $PM_{2.5}$, SO_4^{2-} and NO_3^- were mainly acquired by aqueous phase chemical reactions.

3.2. Sulfur isotopic fractionation during the haze events

3.2.1. Sulfur isotopic compositions of sulfate and SO_2

The regional characteristics of $\delta^{34}S$ value made it meaningful to identify sulfur sources in the atmosphere (Han et al., 2016; Guo et al., 2010). Sulfur isotopic compositions of sulfate and SO_2 during the haze events were determined and the values of $\delta^{34}S\text{-}SO_4^{2-}$ and $\delta^{34}S\text{-}SO_2$ are compared in Fig. 8. It can be observed that the values of $\delta^{34}S\text{-}SO_4^{2-}$ were higher compared to those of $\delta^{34}S\text{-}SO_2$ during the haze events. $\delta^{34}S\text{-}SO_4^{2-}$ values were within the range from 3.7‰ to 6.8‰ with an average and standard deviation at 5.6 ± 1.0‰, while $\delta^{34}S\text{-}SO_2$ values ranged from −0.8‰ to 3.1‰ with an average and standard deviation at 1.5 ± 1.4‰. The discrepancy in the values of $\delta^{34}S\text{-}SO_4^{2-}$ and $\delta^{34}S\text{-}SO_2$ was related to sulfur isotopic fractionation effect during SO_2 oxidation to sulfate. The oxidation of SO_2 resulted in the change of sulfur isotopic composition, which was mainly due to equilibrium or kinetic discrimination between SO_2 and sulfate during the oxidation processes. The influence of different oxidants on sulfur isotopic fractionation needed to be further investigated. It should be pointed out that the variation tendencies of $\delta^{34}S\text{-}SO_4^{2-}$ and $\delta^{34}S\text{-}SO_2$ values were basically consistent indicating that sulfur sources of sulfate and SO_2 in the atmosphere were similar. Guo et al. (2016) determined $\delta^{34}S\text{-}SO_4^{2-}$ values with an average at 4.2‰ during the Youth Olympic Games in Aug. 2014. The discrepancy of $\delta^{34}S\text{-}SO_4^{2-}$ value with this study illustrated different contribution of pollution sources. In addition, we compared the values of $\delta^{34}S\text{-}SO_4^{2-}$ and $\delta^{34}S\text{-}SO_2$ with other cities in China. It is noted there existed an obviously regional difference. The values of $\delta^{34}S\text{-}SO_4^{2-}$ and $\delta^{34}S\text{-}SO_2$ in Nanjing were comparative to those in Shanghai, but lower than those in Beijing and Changchun, higher than those in Guiyang and Wuhan. Generally, the values of $\delta^{34}S\text{-}SO_4^{2-}$ and $\delta^{34}S\text{-}SO_2$ in southern China were lower compared to those in northern China.

According to $\delta^{34}S$ values of potential sulfur sources in Nanjing presented in Fig. 8, $\delta^{34}S$ values of primary sulfate from direct emission of coal combustion, vehicle exhaust and straw burning range from 6.15‰ to 6.63‰, 4.6‰ to 9.7‰ and 5.2 to 7.9‰, respectively (Guo et al., 2016). The average $\delta^{34}S$ value of sulfate in $PM_{2.5}$ was about 5.6‰, which was similar to those from coal combustion. This showed that coal combustion was a sulfur source in $PM_{2.5}$ during the haze events. Besides, the average $\delta^{34}S$ value of sulfate in $PM_{2.5}$ was within the scope of $\delta^{34}S$ from vehicle exhaust and biomass burning, indicating direct emission of these two sources also played a certain role on $PM_{2.5}$. We took 22 Dec. as an example to quantitatively analyze the contributions of coal combustion, vehicle exhaust and biomass burning to $PM_{2.5}$. According to Eq. (1) (Zhang et al., 2010), we obtained that K^+ concentration of non-sea salt ($[K^+_{bb}]$) was 2.87 μg/m^3 on 22 Dec. On this basis, the contribution of biomass burning (f_{bb}%) to $PM_{2.5}$ on 22 Dec. was 8.08% by Eq. (2). Of which, $([K^+_{bb}]/[PM_{2.5}])_{source}$ was 0.15 (Li et al., 2007; Zhang et al., 2007).

$$[K^+_{bb}] = [K^+] - 0.0355[Na^+] \quad (1)$$

$$f_{bb}\% = ([K^+_{bb}]/[PM_{2.5}])_{sample}/([K^+_{bb}]/[PM_{2.5}])_{source} * 100\% \quad (2)$$

Then, the contributions of coal combustion and vehicle exhaust were calculated based on Eqs. (3) and (4) (Han et al., 2016). Considering $\delta^{34}S$ value of sulfate in $PM_{2.5}$ was 6.85‰ on 22 Dec., we calculated the contributions of vehicle exhaust and coal combustion were 50.12% and 41.80%, respectively.

$$\delta^{34}S_{sample} = f_{ve}\delta^{34}S_{ve} + f_{cc}\delta^{34}S_{cc} + f_{bb}\delta^{34}S_{bb} \quad (3)$$

$$f_{ve} + f_{cc} + f_{bb} = 1 \quad (4)$$

where f_{ve}, f_{cc} and f_{bb} represent the contributions of vehicle exhaust, coal combustion and biomass burning, respectively. $\delta^{34}S_{ve}$, $\delta^{34}S_{cc}$ and $\delta^{34}S_{bb}$ are sulfur isotopic values of typical vehicle exhaust, coal combustion and biomass burning in Nanjing region, which were 7.70‰, 6.15‰ and 5.20‰, respectively.

It is noted that the sources of $PM_{2.5}$ based on the study of $\delta^{34}S$ values were in accordance with those from phase clustering analysis of the WSIIs in $PM_{2.5}$. Moreover, $\delta^{34}S$ value showed that primary sulfate made a great contribution to $PM_{2.5}$ during the haze event. It is noted that $\delta^{34}S$ values of sulfate in $PM_{2.5}$ on 23, 25 and 26 Dec. were 4.2‰, 3.7‰ and 4.4‰, respectively, which were lower than the minimum $\delta^{34}S$ value (4.6‰) of primary sulfate from direct emission of potential sources in Nanjing. This indicated that there existed other sulfur sources and the corresponding $\delta^{34}S$ value of sulfate should be lower than 3.7‰. It is reported that $\delta^{34}S$ signature of biogenic sulfur from the organism release in anoxic surface environment to the atmosphere was about −2.4‰ (Mast et al., 2001). High soil moisture and temperature were

the premises for forming anoxic environment in rice farmland near the sampling site. Therefore, low temperature during the haze events made it negligible for the contribution of biogenic sulfur to $PM_{2.5}$. Considering lower $\delta^{34}S$ values of SO_2 in the atmosphere, we speculated low $\delta^{34}S$ values in $PM_{2.5}$ were possibly related to the secondary sulfate from SO_2 oxidation during the haze events.

3.2.2. Heterogeneous and homogeneous oxidation of SO_2

$\delta^{34}S$ value might reflect to formation processes of the secondary sulfate in the atmosphere during SO_2 oxidation due to that $\delta^{34}S$ value may change when SO_2 is converted into sulfate via different homogeneous and heterogeneous oxidation reactions. The measured fractionation with respect to SO_2 is about −9‰ for homogeneous oxidation (Saltzman et al., 1983; Tanaka et al., 1994) and up to +16.5‰ for heterogeneous oxidation (Eriksen, 1972a, 1972b). Assuming sulfate was from SO_2 oxidation and following the mass balance of $\delta^{34}S$ value (Seal, 2006), we might calculate the contribution of SO_2 heterogeneous and homogeneous oxidation to sulfate based on Eqs. (5) and (6).

$$\delta^{34}Sso_2 + 16.5a - 9b = \delta^{34}Sso_4^{2-} \quad (5)$$

$$a + b = 1 \quad (6)$$

where $\delta^{34}Sso_2$, $\delta^{34}Sso_4^{2-}$ are sulfur isotopic compositions of SO_2 and sulfate, respectively. a and b represent the ratio of SO_2 heterogeneous and homogeneous oxidation to sulfate.

It can be observed from Fig. 9 that the contributions of SO_2 heterogeneous and homogeneous oxidation fluctuated significantly during the haze events. SO_2 heterogeneous oxidation predominated on 21 and 22 Dec., however, SO_2 homogeneous oxidation dominated on 23 and 24 Dec. During the period from 25 to 28 Dec., the ratios of heterogeneous oxidation of SO_2 were higher with an average of 53.22%. Besides, we noted that the contribution of SO_2 heterogeneous oxidation reached the maximum value of 58.82% on 30 Dec. Zheng et al. (2015a, 2015b) added heterogeneous reactions to WRF-CMAQ model to evaluate the impact of heterogeneous chemistry and meteorological anomaly on regional haze formation, and found there existed a significant role of heterogeneous chemistry in regional haze formation. In addition, Zheng et al. (2015a, 2015b) observed that heterogeneous reactions played an important role in accelerating production rate of secondary aerosols during the severe pollution event.

The homogeneous oxidation of SO_2 is mainly motivated by OH radicals (Tanaka et al., 1994), while heterogeneous oxidation of SO_2 is related to SO_2 dissolution in cloud and droplet, which was further oxidized by H_2O_2, O_2, O_3 and NO_2 (Hung and Hoffmann, 2015; He et al., 2014; Harris et al., 2013; Eriksen, 1972b). Cheng et al. (2016) investigated sulfate production during Jan. 2013 winter haze event in Beijing, and found that the missing source of sulfate and particulate matter could be explained by reactive nitrogen chemistry in aerosol water. According to Table 1, high O_3 concentration on 21 Dec. was favorable for heterogeneous oxidation of SO_2. Besides, the relatively high NO_2 concentration and RH accelerated SO_2 heterogeneous oxidation. Different from that on 21 Dec., large amount of sulfate was produced mainly by SO_2 heterogeneous oxidation in the presence of the highest NO_2 concentration on 22 Dec. On the contrary, low O_3 and NO_2 concentrations inhibited SO_2 heterogeneous oxidation to sulfate on 23 and 24 Dec. although there existed the highest RH in the atmosphere. Similarly, high ratios of SO_2 heterogeneous and homogeneous oxidation on 25, 26 and 30 Dec. were ascribed to high RH and O_3 concentration as well as high NO_2 concentration. Especially, very low A/C value (0.66) on 30 Dec. indicated the strong alkaline of $PM_{2.5}$, thereby further promoting SO_2 heterogeneous oxidation in the presence of O_3 and NO_2. Considering the solubility of SO_2 decreased with the increase of temperature, we inferred that the temperature might exert an influence on heterogeneous oxidation. It is noteworthy that the maximum temperature on 28 and 30 Dec. were 6 °C and 12 °C. However, the corresponding contributions of SO_2 heterogeneous oxidation were 54.0% and 58.8%, respectively. Compared with the temperature, we believed the concentrations of gaseous pollutants, A/C value and RH were the more important factors in affecting SO_2 heterogeneous oxidation.

4. Conclusions

There was presence of serious $PM_{2.5}$ pollution during the haze events, and the pollutants were mainly from coal combustion, vehicle exhaust release and biomass burning. The contributions of coal combustion, vehicle exhaust and biomass burning to $PM_{2.5}$ on 22 Dec. were 41.80%, 50.12% and 8.08%, respectively. The secondary sulfate in $PM_{2.5}$ was ascribed to aqueous phase sulfur oxidation promoted by high NO_2 concentration and RH under the alkaline condition. According to sulfur isotopic fractionation between $\delta^{34}S\text{-}SO_4^{2-}$ and $\delta^{34}S\text{-}SO_2$, we calculated that the average contribution of SO_2 heterogeneous oxidation to sulfate was about 48.8% during the haze events.

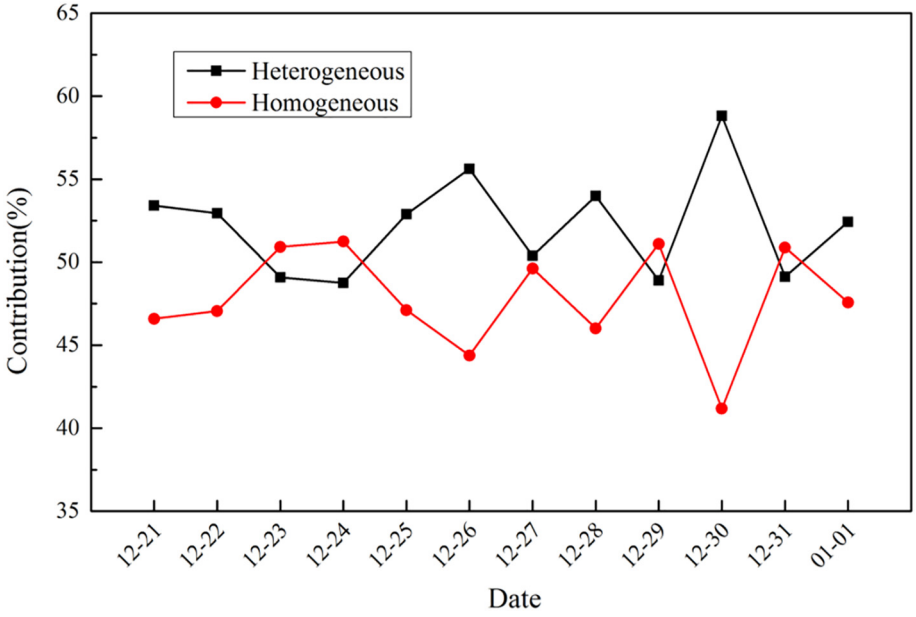

Fig. 9. The contribution of SO_2 heterogeneous and homogeneous oxidation to sulfate.

Acknowledgments

We gratefully acknowledge supports from National Natural Science Foundation of China (41873016, 41625006, 91544229-02, 41373023); Jiangsu Province "333 Talent Project"; Sponsored by Jiangsu Province "Qing Lan Project"; A Project Funded by Priority Academic Program Development of Jiangsu Higher Education Institutions.

References

Arimoto, R., Duce, R.A., Savoie, D.L., Prospero, J.M., Talbot, R., Cullen, J.D., Tomza, U., Lewis, N.F., Ray, B.J., 1996. Relationships among aerosol constituents from Asia and the North Pacific during PEM-West A. J. Geophys. Res. Atmos. 101, 2011–2023.

Cai, S., Wang, Y., Zhao, B., Wang, S., Chang, X., Hao, J., 2017. The impact of the "Air Pollution Prevention and Control Action Plan" on $PM_{2.5}$ concentrations in Jing-Jin-Ji region during 2012–2020. Sci. Total Environ. 580, 197–209.

Chen, J., Zhao, C.S., Ma, N., Liu, P.F., Gobel, T., Hallbauer, E., Deng, Z.Z., Ran, L., Xu, W.Y., Liang, Z., Liu, H.J., Yan, P., Zhou, X.J., Wiedensohler, A., 2012. A parameterization of low visibilities for hazy days in the North China Plain. Atmos. Chem. Phys. 12 (11), 4935–4950.

Cheng, Z., Wang, S.X., Jiang, J.K., Fu, Q.Y., Chen, C.H., Xu, B.Y., Yu, J.Q., Fu, X., Hao, J.M., 2013. Long-term trend of haze pollution and impact of particulate matter in the Yangtze River Delta, China. Environ. Pollut. 182, 101–110.

Cheng, Y., Lee, S.C., Gu, Z.L., Ho, K.F., Zhang, Y.W., Huang, Y., Chow, J.C., Waston, J.G., Cao, J.J., Zhang, R.J., 2015. $PM_{2.5}$ and $PM_{10-2.5}PM_{10-2.5}$ chemical composition and source apportionment near a Hong Kong roadway. Particuology 18, 96–104.

Cheng, Y.F., Zheng, G.J., Wei, C., Mu, Q., Zheng, B., Wang, Z.B., Gao, M., Zhang, Q., He, K.B., Carmichael, G., Poschl, U., Su, H., 2016. Reactive nitrogen chemistry in aerosol water as a source of sulfate during haze events in China. Sci. Adv. 2 (12), e1601530.

China Meteorological Administration, 2010. China Meteorological Administration Observation and Forecasting Levels of Haze (QX/T113–2010). (in Chinese).

Cong, Z.Y., Kang, S.C., Luo, C.L., Li, Q., Huang, J., Gao, S.P., Li, X.D., 2011. Trace elements and lead isotopic composition of PM_{10} in Lhasa, Tibet. Atmos. Environ. 45, 6210–6215.

Cuhadaroglu, B., Demirci, E., 1997. Influence of some meteorological factors on air pollution in Trabzon city. Energy Build. 25 (3), 179–184.

Duo, B., Zhang, Y.C., Kong, L.D., Fu, H.B., Hu, Y.J., Chen, J.M., Li, L., Qiong, A., 2015. Individual particle analysis of aerosols collected at Lhasa City in the Tibetan plateau. J. Environ. Sci. 29, 165–177.

Eriksen, T.E., 1972a. Sulfur isotope effects 1. Isotopic exchanges coefficient for sulfur isotopes ^{34}S-^{32}S in system $SO_{2(g)}$-$HSO_{3(aq)}$ at 25, 35 and 45 Degrees C. Acta Chem. Scand. 26, 573.

Eriksen, T.E., 1972b. Sulfur isotope effects 2. Isotopic exchanges coefficient for sulfur isotopes ^{34}S-^{32}S in system $SO_{2(g)}$-aqueous solutions of SO_2. Acta Chem. Scand. 26, 581.

Feng, J.L., Yu, H., Su, X.F., Liu, S.H., Li, Y., Pan, Y.P., Sun, J.H., 2016. Chemical composition and source apportionment of $PM_{2.5}$ during Chinese Spring Festival at Xinxiang, a heavily polluted city in North China: Fireworks and health risks. Atmos. Res. 182, 176–188.

Gao, J.J., Tian, H.Z., Cheng, K., Lu, L., Zheng, M., Wang, S.X., Hao, J.M., Wang, K., Hua, S.B., Zhu, C.Y., Wang, Y., 2015. The variation of chemical characteristics of $PM_{2.5}$ and PM_{10} and formation causes during two haze pollution events in urban Beijing, China. Atmos. Environ. 107 (1–8).

Ge, X., Wexler, A.S., Clegg, S.L., 2011. Atmospheric amines-Part 1. A review. Atmos. Environ. 45 (3), 524–546.

Guo, Z.B., Li, Z.Q., Farquhar, J., Kaufman, A.J., Wu, N.P., Li, C., Dickerson, R.R., Wang, P.C., 2010. Identification of sources and formation processes of atmospheric sulfate by sulfur isotope and scanning electron microscope measurements. J. Geophys. Res.-Atmos. 115. https://doi.org/10.1029/2009JD012893.

Guo, Z.B., Wu, M.L., Liu, F.L., Wei, Y., Li, D.F., 2014. Multiple sulfur and oxygen isotope compositions in Beijing aerosol. Sci. China Earth Sci. 57 (11), 2671–2675.

Guo, Z.B., Shi, L., Chen, S.L., Jiang, W.J., Wei, Y., Rui, M.L., Zeng, G., 2016. Sulfur isotopic fractionation and source apportionmentof $PM_{2.5}$ in Nanjing region around the second session of the Youth Olympic Games. Atmos. Res. 174-175, 9–17.

Guo, H.Y., Weber, R.J., Nenes, A., 2017. High levels of ammonia do not raise fine particle pH sufficiently to yield nitrogen oxide-dominated sulfate production. Sci. Rep. 12109. https://doi.org/10.1038/s41598-017-11704-0.

Han, X.K., Guo, Q.J., Liu, C.Q., Fu, P.Q., Strauss, H., Yang, J.X., Hu, J., Wei, L.F., Ren, H., Peters, M., Wei, R.F., Tian, L.Y., 2016. Using stable isotopes to trace sources and formation processes of sulfate aerosols from Beijing, China. Sci. Rep. 6, 29958. https://doi.org/10.1038/srep29958.

Harris, E., Sinha, B., Tilgner, A., Fomba, K.W., 2013. Enhanced role of transition metal ion catalysis during in-cloud oxidation of SO_2. Science 340, 727–730.

Hassan, S.K., Khoder, M.I., 2017. Chemical characteristics of atmospheric $PM_{2.5}$ loads during air pollution episodes in Giza, Egypt. Atmos. Environ. 150, 346–355.

He, H., Wang, Y.S., Ma, Q.X., Ma, J.Z., Chu, B.W., Ji, D.S., Tang, G.Q., Liu, C., Zhang, H.X., Hao, J.M., 2014. Mineral dust and NO_x promote the conversion of SO_2 to sulfate in heavy pollution days. Sci. Rep. 4, 4172. https://doi.org/10.1038/srep06092.

Hu, G.Y., Zhang, Y.M., Sun, J.Y., Zhang, L.M., Shen, X.J., Lin, W.L., Yang, Y., 2014. Variability, formation and acidity of water-soluble ions in $PM_{2.5}$ in Beijing based on the semi-continuous observations. Atmos. Res. 145-146, 1–11.

Hung, H.-M., Hoffmann, M.R., 2015. Oxidation of gas-phase SO2 on the surfaces of acidic microdroplets: Implications for sulfate and sulfate radical anion formation in the atmospheric liquid phase. Environ. Sci. Technol. 49 (23), 13768–13776.

Jiang, M.J., Li, Z.Q., Wan, B.C., Cribb, M., 2016. Impact of aerosols on precipitation from deep convective clouds in eastern China. J. Geophys. Res. Atmos. 121 (16), 9607–9620.

Kang, C.M., Lee, H.S., Kang, B.W., Lee, S.K., Sunwoo, Y., 2004. Chemical characteristics of acidic gas pollutants and $PM_{2.5}$ species during hazy episodes in Seoul, South Korea. Atmos. Environ. 38, 4749–4760.

Karthikeyan, S., Balasubramanian, R., 2006. Determination of water-soluble inorganic and organic species in atmospheric fine particulate matter. Microchem. J. 82, 49–55.

Kong, S.F., Li, X.X., Li, L., Yin, Y., Chen, K., Yuan, L., Zhang, Y.J., Shan, Y.P., Ji, Y.Q., 2015. Variation of polycyclic aromatic hydrocarbons in atmospheric $PM_{2.5}$ during winter haze period around 2014 Chinese Spring Festival at Nanjing: insights of source changes, air mass direction and firework particle injection. Sci. Total Environ. 520, 59–72.

Leung, F.Y., Colussi, A., Hoffmanm, M., 2001. Sufur isotopic fractionation in the gas-phase oxidation of sulfur dioxide initiated by hydroxyl radicals. J. Phys. Chem. A 105 (34), 8073–8076.

Li, X.H., Lei, S.W., An, D., 2007. Particulate and trace gas emissions from open burning of wheat straw and corn stover in China. Environ. Sci. Technol. 41, 6052–6058.

Lu, Z., Streets, D.G., Zhang, Q., Wang, S., Carmichael, G.R., Cheng, Y.F., Wei, C., Chin, M., Diehl, T., Tan, Q., 2010. Sulfur dioxide emissions in China and sulfur trends in East Asia since 2000. Atmos. Chem. Phys. 10, 6311–6331.

Li, H.M., Wang, Q.G., Yang, M., Li, F.Y., Wang, J.H., Sun, Y.X., Wang, C., 2016. Chemical characterization and source apportionment of $PM_{2.5}$ aerosols in a megacity of Southeast China. Atmos. Res. 181, 288–299.

Mast, M.A., Turk, J.T., Ingersoll, G.P., Clow, D.W., Kester, C.L., 2001. Use of stable sulfur isotopes to identify sources of sulfate in Rocky Mountain snowpacks. Atmos. Environ. 35 (19), 3303–3313.

Ohizumi, T., Take, N., Inomata, Y., Yagoh, H., Endo, T., Takahashi, M., Yanahara, K., Kusakabe, M., 2014. Long-term variation of the source of sulfate deposition in a leeward area of Asian continent in view of sulfur isotopic composition. Atmos. Environ. 140, 42–51.

Pastuszka, J.S., Wawroś, A., Talik, E., Paw, U.K.T., 2003. Optical and chemical characteristics of the atmospheric aerosol in four towns in southern Poland. Sci. Total Environ. 309, 237–251.

Peng, J.F., Hu, M., Guo, S., Du, Z.F., Zheng, J., Shang, D.J., Zamora, M.L., Zeng, L.M., Shao, M., Wu, Y.S., 2016. Markedly enhanced absorption and direct radiative forcing of black carbon under polluted urban environments. Proc. Natl. Acad. Sci. U. S. A. 113 (16), 4266–4271.

Sakata, M., Ishikawa, T., Mitsunobu, S., 2013. Effectiveness of sulfur and boron isotopes in aerosols as tracers of emissions from coal burning in Asian continent. Atmos. Environ. 67, 296–303.

Saltzman, E.S., Brass, G., Price, D., 1983. The mechanism of sulfate aerosol formation: chemical and sulfur isotopic evidence. Geophys. Res. Lett. 10, 513–516.

Sarwar, G., Fahey, K., Kwok, R., Gilliam, R.C., Roselle, S.J., Mathur, R., Xue, J., Yu, J.Z., Carter, W.P.L., 2013. Potential impacts of two SO_2 oxidation pathways on regional sulfate concentrations: Aqueous-phase oxidation by NO_2 and gas-phase oxidation by Stabilized Criegee Intermediates. Atmos. Environ. 68, 186–197.

Seal, R.R., 2006. Sulfur isotope geochemistry of sulfide minerals. Rev. Mineral. Geochem. 61, 633–677.

Seinfeld, J.H., Pandis, S.N., 1998. Atmospheric Chemistry and Physics. Wiley & Sons, New York, USA, pp. 363–379.

Shen, X.J., Sun, J.Y., Zhang, X.Y., Zhang, Y.M., Zhang, L., Che, H.C., Ma, Q.L., Yu, X.M., Yue, Y., Zhang, Y.W., 2015. Characterization of submicron aerosols and effect on visibility during a severe haze-fog episode in Yangtze River Delta, China. Atmos. Environ. 120, 307–316.

Sinha, B., Hoppe, P., Huth, J., Foley, S., Andreae, M., 2008. Sulfur isotope analyses of individual aerosol particles in the urban aerosol at a central European site (Mainz, Germany). Atmos. Chem. Phys. 8, 7271–7288.

Sun, Z.Q., Mu, Y.J., Liu, Y.J., Shao, L.Y., 2013. A comparison study on airborne particles during haze days and non-haze days in Beijing. Sci. Total Environ. 456-457, 1–8.

Tan, J.H., Duan, J.C., Zhen, N.J., He, K.B., Hao, J.M., 2016. Chemical characteristics and source of size-fractionated atmospheric particle in haze episode in Beijing. Atmos. Res. 167, 24–33.

Tanaka, N., Rye, D.M., Xiao, Y., Lassaga, A.C., 1994. Use of stable sulfur isotope systematic for evaluating oxidation reaction pathways and in-cloud scavenging of sulfur dioxide in the atmosphere. Geophys. Res. Lett. 21 (4), 1519–1522.

Tao, J., Zhang, L.M., Ho, K.F., Zhang, R.J., Lin, Z.J., Zhang, Z.S., Lin, M., Cao, J.J., Liu, S.X., Wang, G.H., 2014. Impact of $PM_{2.5}$ chemical compositions on aerosol light scattering in Guangzhou-the largest megacity in South China. Atmos. Res. 135–136, 48–58.

Ueda, S., Miura, K., Kawata, R., Furutani, H., Uematsu, M., Omori, Y., Tanimoto, H., 2016. Number-size distribution of aerosol particles and new particle formation events in tropical and subtropical Pacific Oceans. Atmos. Environ. 142, 324–339.

Wang, G.H., Chen, C.L., Li, J.J., Zhou, B.H., Xie, M.J., Hu, S.Y., Kawamura, K., Chen, Y., 2011. Molecular composition and size distribution of sugars, sugar-alcohols and carboxylic acids in airborne particles during a severe urban haze event caused by wheat straw burning. Atmos. Environ. 45, 2473–2479.

Wang, H., Zhu, B., Shen, L., Kang, H., 2012. Size distributions of aerosol and water-soluble ions in Nanjing during a crop residual burning event. J. Environ. Sci. 24, 1457–1465.

Wang, P., Cao, J.J., Shen, Z.X., Han, Y.M., Lee, S.C., Huang, Y., Zhu, C.S., Wang, Q.Y., Xu, H.M., Huang, R.J., 2015. Spatial and seasonal variations of $PM_{2.5}$ mass and species during 2010 in Xi'an, China. Sci. Total Environ. 508, 477–487.

Wang, G.H., Zhang, R.Y., Gomez, M.E., Yang, L.X., Zamora, M.L., Hu, M., Lin, Y., Peng, J.F., Guo, S., Meng, J.J., Li, J.J., Cheng, C.L., Hu, T.F., Wang, Y.S., Cao, J.J., An, Z.S.,

et al., 2016. Persistent sulfate formation from London fog to Chinese haze. In: Proceedings of the National Academy of Sciences of the United States of America, https://doi.org/10.1073/pnas.1616540113.
Wang, H.B., Shi, G.M., Tian, M., Zhang, L.M., Chen, Y., Yang, F.M., Cao, X.Y., 2017a. Aerosol optical properties and chemical composition apportionment in Sichuan Basin, China. Sci. Total Environ. 577, 245–258.
Wang, J., Zhao, B., Wang, S., Yang, F., Xing, J., Morawska, L., Ding, A., Kulmala, M., Kerminen, V.M., Kujansuu, J., Wang, Z., Ding, D., Zhang, X., Wang, H., Tian, M., Petäjä, T., Jiang, J., Hao, J., 2017b. Particulate matter pollution over China and the effects of control policies. Sci. Total Environ. 584-585, 426–447.
Xiao, H.W., Xiao, H.Y., Long, A.M., Wang, Y.L., Liu, C.Q., 2014. Sources and meteorological factors that control seasonal variation of $\delta^{34}S$ values in rainwater. Atmos. Res. 149, 154–165.
Xie, Y.N., Ding, A.J., Nie, W., Mao, H.T., Qi, X.M., Huang, X., Xu, Z., Kerminen, V.M., Petaja, T., 2015. Enhanced sulfate formation by nitrogen dioxide: implications from in situ observations at the SORPES station. J. Geophys. Res.-Atmos. 120, 12679–12694.
Yang, Z., Li, X.D., Deng, J., Wang, H.Y., 2015. Stable sulfur isotope ratios and water-soluble inorganic compositions of PM_{10} in Yichang City, central China. Environ. Sci. Pollut. Res. 22, 13564–13572.
Yuan, Q., Li, W.J., Zhou, S.Z., Yang, L.X., Chi, J.W., Sui, X., Wang, W.X., 2015. Integrated evaluation of aerosols during haze-fog episodes at one regional background site in North China Plain. Atmos. Res. 156, 102–110.
Zhang, Y.X., Shao, M., Zhang, Y.H., 2007. Source profiles of particulate organic matters emitted from cereal straw burnings. Environ. Sci. 19, 167–175.
Zhang, Z.S., Engling, G., Lin, C.Y., 2010. Chemical speciation, transport and contribution of biomass burning smoke to ambient aerosol in Guangzhou, a mega city of China. Atmos. Environ. 44, 3187–3195.
Zhang, F.W., Xu, L.L., Chen, J.S., Yu, Y.K., Niu, Z.C., Yin, L.Q., 2012. Chemical compositions and extinction coefficients of $PM_{2.5}$ in peri-urban of Xiamen, China, during June 2009-May 2010. Atmos. Res. 106, 150–158.
Zhang, R.Y., Wang, G.H., Guo, S., Zarnora, M.L., Ying, Q., Lin, Y., Wang, W.G., Hu, M., Wang, Y., 2015. Formation of urban fine particulate matter. Chem. Rev. 115 (10), 3803–3855.
Zheng, G.J., Duan, F.K., Su, H., Ma, Y.L., Cheng, Y., Zheng, B., Zhang, Q., Huang, T., Kimoto, T., Chang, D., Poschl, U., Cheng, Y.F., He, K.B., 2015a. Exploring the severe winter haze in Beijing: the impact of synoptic weather, regional transport and heterogeneous reactions. Atmos. Chem. Phys. 15 (6), 2969–2983.
Zheng, B., Zhang, Q., Zhang, Y., He, K.B., Wang, K., Zheng, G.J., Duan, F.K., Ma,Y.L., Kimoto, T., 2015b. Heterogeneous chemistry: a mechanism missing in current models to explain secondary inorganic aerosol formation during the January 2013 haze episode in North China. Atmos. Chem. Phys. 15(4), 2031–2049.
Zhou, J.B., Xing, Z.Y., Deng, J.J., Du, K., 2016. Characterizing and sourcing ambient $PM_{2.5}$ over key emission regions in China I: water-soluble ions and carbonaceous fractions. Atmos. Environ. 135, 20–30.